Identification of *Burkholderia cenocepacia* Genes Required for Bacterial Survival In Vivo

Tracey A. Hunt,[1]† Cora Kooi,[2] Pamela A. Sokol,[2] and Miguel A. Valvano[1,3]*

*Departments of Microbiology and Immunology[1] and Medicine,[3] University of Western Ontario, London,
Ontario N6A 5C1, and Department of Microbiology and Infectious Diseases, University of
Calgary Health Sciences Centre, Calgary, Alberta T2N 4N1,[2] Canada*

Burkholderia cenocepacia* (formerly *Burkholderia cepacia* complex genomovar III) causes chronic lung infections in patients with cystic fibrosis. In this work, we used a modified signature-tagged mutagenesis (STM) strategy for the isolation of *B. cenocepacia* mutants that cannot survive in vivo. Thirty-seven specialized plasposons, each carrying a unique oligonucleotide tag signature, were constructed and used to examine the survival of 2,627 *B. cenocepacia* transposon mutants, arranged in pools of 37 unique mutants, after a 10-day lung infection in rats by using the agar bead model. The recovered mutants were screened by real-time PCR, resulting in the identification of 260 mutants which presumably did not survive within the lungs. These mutants were repooled into smaller pools, and the infections were repeated. After a second screen, we isolated 102 mutants unable to survive in the rat model. The location of the transposon in each of these mutants was mapped within the *B. cenocepacia* chromosomes. We identified mutations in genes involved in cellular metabolism, global regulation, DNA replication and repair, and those encoding bacterial surface structures, including transmembrane proteins and cell surface polysaccharides. Also, we found 18 genes of unknown function, which are conserved in other bacteria. A subset of 12 representative mutants that were individually examined using the rat model in competition with the wild-type strain displayed reduced survival, confirming the predictive value of our STM screen. This study provides a blueprint to investigate at the molecular level the basis for survival and persistence of *B. cenocepacia* within the airways.

Isolates of the *Burkholderia cepacia* complex are gram-negative opportunistic pathogens. Usually harmless while surviving in the soil, these bacteria can cause devastating infections in patients with cystic fibrosis (CF) and chronic granulomatous disease (3, 23, 24, 30, 31). *Pseudomonas aeruginosa* is the predominant respiratory pathogen in CF patients (23), but the disease risk for infection with *B. cepacia* complex in patients with CF is substantially higher than with *P. aeruginosa* alone or with other bacteria (13). Although the clinical outcome among CF patients infected with *B. cepacia* complex varies greatly, infections in some patients result in a rapidly progressive and fatal bacteremic disease (30). Furthermore, isolates of the *B. cepacia* complex have the potential for patient-to-patient spread, both within and outside the hospital (22, 32, 41, 51, 52). Recent taxonomic studies demonstrated that strains identified as *B. cepacia* comprise a complex of closely related species or genomovars, collectively called the *B. cepacia* complex (43, 67). This complex consists of at least nine species sharing a high degree of 16S rDNA and *recA* sequence similarity and moderate levels of DNA-DNA hybridization (for a recent review, see reference 10). Strains of each of the species within the *B. cepacia* complex have been isolated from CF patients; however, some are more common than others. *Burkholderia multivorans* (formerly genomovar II) and *Burkholderia cenocepacia*

(formerly genomovar III) isolates comprise about 10 and 83%, respectively, of all *B. cepacia* complex isolated from CF patients in Canada (62).

Isolates of the *B. cepacia* complex are inherently resistant to many antimicrobial agents (49, 54, 55). The widespread antibiotic resistance of these microorganisms has proven extremely problematic for the treatment of infections. Furthermore, the lack of sensitivity to antibiotics commonly used for genetic selection complicates genetic studies in this pathogen by drastically limiting the choice of antibiotic resistance gene markers for mutagenesis and complementation experiments (38).

Several bacterial factors may play a role in the infections caused by isolates of the *B. cepacia* complex. Some isolates have the ability to survive intracellularly within eukaryotic cells such as macrophages, respiratory epithelial cells, and amoebae (6, 34, 44, 46, 56). Other potential virulence factors that have been described include cable pili (57), flagella (65), a type III secretion system (50, 64), surface exopolysaccharide (7, 9), production of melanin (71), catalase (37), up to four types of iron-chelating siderophores (16), proteases and other secreted enzymes (12, 29, 47, 68), quorum-sensing systems (40, 42), and the ability to form biofilms (66). Not all strains produce each of the proposed virulence factors and, to date, none of these individual factors has been clearly demonstrated to be a major contributor to human disease.

Signature-tagged mutagenesis (STM) was originally developed to facilitate the detection of *Salmonella enterica* serovar Typhimurium genes required for in vivo survival (28). STM has since been applied to several different bacteria and fungal pathogens (for a recent review, see reference 48). STM is a comparative hybridization technique that employs a collection

* Corresponding author. Present address: Department of Microbiology and Immunology, Dental Sciences Building, Rm. 3014, University of Western Ontario, London, Ontario N6A 5C1, Canada. Phone: (519) 661-3996. Fax: (519) 661-3499. E-mail: mvalvano@uwo.ca.
† Present address: Department of Cell Biology, University of Alberta, Edmonton, Alberta T6G 2H7, Canada.

of transposons, each modified by the incorporation of a unique DNA sequence tag (28). These transposons are introduced into the pathogen to be studied and, following random transposition, insertional mutants are isolated. Mutants containing a transposon insertion in a gene which codes for a function required for in vivo growth or survival will fail to pass through the in vivo selection. Individual mutants can be distinguished from each other based on unique tags carried by the transposon insertions of each strain. By comparing the tags present in the input pool of mutants initially inoculated into the animal model with those unique tags present in the bacteria recovered after infection, it is possible to identify mutants that fail to grow exclusively in vivo. Subsequently, the DNA sequence surrounding the insertion can be analyzed to identify the gene or genes required for virulence. Traditional STM involves using randomly generated tags that can be detected by conventional hybridization techniques (28), which may result in cross-hybridization signals and high background, increasing the proportion of false positives (53). This was a significant concern in the case of *B. cenocepacia* due to the high moles percent G+C content of the genome. A PCR-based modification of STM can potentially eliminate pitfalls inherent to hybridization and increase the specificity during the PCR screening step (39).

In this study, we describe a modified STM procedure to isolate and identify candidate genes of *B. cenocepacia* required for the in vivo survival in 102 transposon mutants that could not be recovered from intratracheal lung infections in rats. The modifications to the STM strategy included the use of a real-time PCR-based screening step for the detection of each transposon mutant within a pool. In addition, we used a plasposon backbone instead of a classical transposon to facilitate the identification of flanking chromosomal regions once the element is integrated onto the chromosome, since the transposable element within the plasposon contains an *Escherichia coli* plasmid replication origin (18). Inherent problems of STM such as cross-amplifying tags were removed prior to preparing the pools for the in vivo passage, thereby making these modifications useful as a general screening method to identify genes required for survival in vivo.

MATERIALS AND METHODS

Bacterial strains and growth conditions. Unless otherwise indicated, all strains were grown at 37°C. *B. cenocepacia* strain K56-2 (16) was grown in Luria-Bertani (LB) medium. This strain is a CF isolate that belongs to the same clonal group as the strain J2315, whose genome has recently been sequenced (http://www .sanger.ac.uk/Projects/B_cenocepacia/), and it was previously shown to cause a chronic lung infection in the agar bead rat model (61). *E. coli* DH5α [F⁻ φ80 lacZΔM15 endA1 recA1 hsdR17(r_K^- m_K^+) supE44 thi-1 ΔgyrA96 (ΔlacZYA-argF)U169 relA1] was used as a host for the plasposon constructs and for the helper plasmid pRK2013 (see below). Transposon mutants were grown in Typticase soy agar, Vogel-Bonner minimal medium (VBM) (69), or LB medium as required, all of which were supplemented with trimethoprim at a final concentration of 100 μg/ml. *E. coli* strains were grown in LB medium supplemented with 50 μg of trimethoprim/ml or 40 μg of kanamycin/ml, as appropriate. All chemicals were purchased from Sigma Chemical Co., St. Louis, Mo., unless otherwise indicated.

Construction of a library of plasposons carrying unique oligonucleotide tags. Forty-one plasposons (designated pTn*Mod*-OTp-tag1 to pTn*Mod*-OTp-tag41) were constructed as depicted in Fig. 1. The plasposon backbone was from pTn*Mod*-OTp′ (18). Forty-one different oligonucleotides of 21 bp (Table 1) were annealed to complementary molecules to yield double-stranded oligonucleotides. The ends of the double-stranded oligonucleotides were phosphorylated
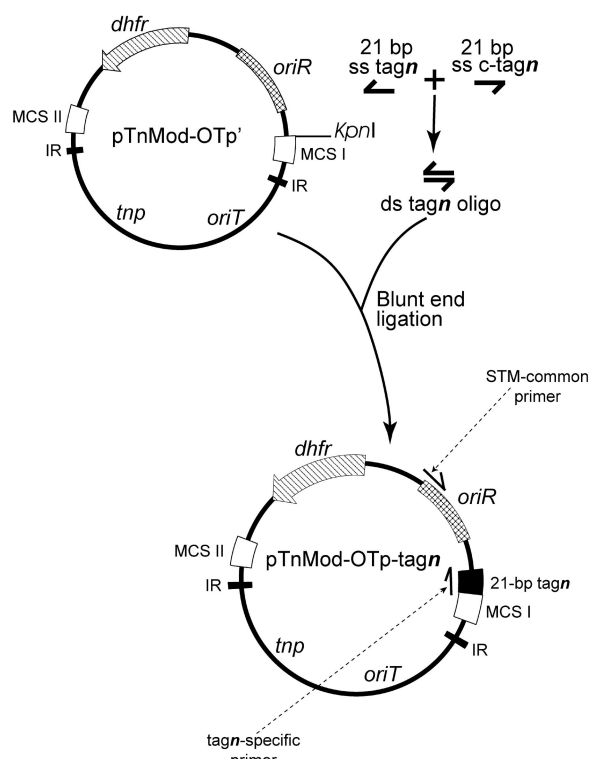

FIG. 1. Construction of the tag plasposons. The transposons pTn*Mod*-OTp-tag*n* were constructed using the backbone of pTn*Mod*-OTp′ by digesting this plasposon at the unique KpnI site and blunting the ends. The KpnI site was chosen because it is located in one of the two multiple cloning sites (MCS) within the inverted repeats (IR) and therefore within the transposable element portion of the plasposon. The 21-bp tag oligonucleotides (tag*n*) were separately annealed to the complementary sequences (c-tag*n*), and the ends were phosphorylated. The double-stranded oligonucleotides were separately blunt-end ligated into the blunted KpnI site to yield the plasposons pTn*Mod*-OTp-tag*n*. This procedure was followed for each of the 41 tags. *oriR* is the *E. coli* origin of replication, *dhfr* is the trimethoprim resistance cassette, *tnp* is the transposase, and *oriT* is the origin of transfer. Arrows in pTn*Mod*-OTp-tag*n* denote the location of the STM common primer (STM-common) and the tag*n*-specific primers used for PCR amplifications. ds, double stranded; ss, single stranded.

and separately ligated into the blunted KpnI site of pTn*Mod*-OTp′ to produce 41 different plasposons pTn*Mod*-OTp-tag*n*, where *n* is the oligonucleotide tag number 1 to 41. Ligations were verified by PCR using each of the 21-bp oligonucleotides (Table 1) as one primer and primer STM-common (5′-TCGATTT CGTTCCACTGAGCG-3′) as the second primer. PCR amplifications were performed in a PTC-0200 DNA engine (MJ Research, Incline Village, Nev.) by using *Taq* polymerase (Roche Diagnostics, Laval, Quebec, Canada). The 811-bp product was amplified as follows: 7 min at 95°C, two cycles of 95°C for 1 min, 65°C for 2 s (followed by decreases of 0.2°C per second up to 55°C), and 72°C for 1 min; and then 10 cycles of 95°C for 1 min, 55°C for 1 min, and 72°C for 1 min. The product was visualized on a 0.7% (wt/vol) agarose gel.

Transposon mutant library. Transposon mutagenesis of *B. cenocepacia* K56-2 was performed 41 separate times using each pTn*Mod*-OTp-tag*n* plasposon to produce 96 individual K56-2 transposon mutants for each tagged transposon. Triparental matings were carried out as previously reported (15) to mobilize each plasposon into K56-2 with *E. coli* DH5α(pRK2013) as a helper strain (21). After transposition, insertion mutants were plated on minimal VBM media supplemented with trimethoprim to prevent the recovery of auxotrophic mutants, and finally the individual mutants were stored in 96-well plates.

Animal infections. Infections were done using the agar bead model of chronic lung infection in rats as previously described (61). Two Sprague-Dawley male rats (150 to 160 g; Charles River Canada) were used for each infection pool of 37 *B. cenocepacia* transposon mutants containing 10^5 viable bacteria embedded

TABLE 1. Nucleotide sequences of tags for STM

Tag no.	Sequence[a]
tag1	5′-GTACCGCGCTTAA**ACGTTCA**G-3′
tag2	5′-GTACCGCGCTTAA**ATAGCCT**G-3′
tag3	5′-GTACCGCGCTTAA**AAGTCTC**G-3′
tag4	5′-GTACCGCGCTTAA**TAACGTG**G-3′
tag5	5′-GTACCGCGCTTAA**ACTGGTA**G-3′
tag6	5′-GTACCGCGCTTAA**GCATGTT**G-3′
tag7	5′-GTACCGCGCTTAA**TGTAACC**G-3′
tag8	5′-GTACCGCGCTTAA**AATCTCG**G-3′
tag9	5′-GTACCGCGCTTAA**TAGGCAA**G-3′
tag10	5′-GTACCGCGCTTAA**CAATCGT**G-3′
tag11	5′-GTACCGCGCTTAA**TCAAGAC**G-3′
tag12	5′-GTACCGCGCTTAA**CTAGTAG**G-3′
tag13[b]	5′-GTACCGCGCTTAA**ACGTTCA**G-3′
tag14	5′-GTACCGCGCTTAA**TGACATG**G-3′
tag15	5′-GTACCGCGCTTAA**TACTGGA**G-3′
tag16	5′-GTACCGCGCTTAA**GTTCACT**G-3′
tag17	5′-GTACCGCGCTTAA**ATGCAGA**G-3′
tag18	5′-GTACCGCGCTTAA**CATAGCT**G-3′
tag19	5′-GTACCGCGCTTAA**AGTAGAG**G-3′
tag20	5′-GTACCGCGCTTAA**GTACCTA**G-3′
tag21[b]	5′-GTACCGCGCTTAA**TAGAGCA**G-3′
tag22	5′-GTACCGCGCTTAA**CCTAGAT**G-3′
tag23	5′-GTACCGCGCTTAA**CTACTGT**G-3′
tag24[b]	5′-GTACCGCGCTTAA**GTAACAG**G-3′
tag25	5′-GTACCGCGCTTAA**TGAACTC**G-3′
tag26	5′-GTACCGCGCTTAA**GGTATCA**G-3′
tag27	5′-GTACCGCGCTTAA**CGAACTA**G-3′
tag28	5′-GTACCGCGCTTAA**CTGACAT**G-3′
tag29	5′-GTACCGCGCTTAA**TCTGATG**G-3′
tag30[b]	5′-GTACCGCGCTTAA**TTGACGT**G-3′
tag31	5′-GTACCGCGCTTAA**CTGTGAA**G-3′
tag32	5′-GTACCGCGCTTAA**CTGTATGA**G-3′
tag33	5′-GTACCGCGCTTAA**TCGAATC**G-3′
tag34	5′-GTACCGCGCTTAA**CATGCTT**G-3′
tag35	5′-GTACCGCGCTTAA**GATATCG**G-3′
tag36	5′-GTACCGCGCTTAA**CAGTTGA**G-3′
tag37	5′-GTACCGCGCTTAA**CGTATGT**G-3′
tag38	5′-GTACCGCGCTTAA**GTATCAC**G-3′
tag39	5′-GTACCGCGCTTAA**ATATCGC**G-3′
tag40	5′-GTACCGCGCTTAA**ACTACTG**G-3′
tag41	5′-GTACCGCGCTTAA**CTAGAAC**G-3′

[a] The constant region is shown in normal font and the 7-bp variable region is in bold. The 5′ sequence is conserved for each tag to facilitate the binding of the primers to the template during the annealing step while the variable region is at the 3′ end to give specificity during the elongation step of the PCR reaction.

[b] Tags that cross-reacted with other tags which were eliminated from the study.

in agar beads. The lungs were removed 10 days following intratracheal instillation into the left pulmonary lobe and homogenized using a Polytron homogenizer (Brinkman Instruments, Westbury, N.Y.). Serial dilutions in phosphate-buffered saline were plated on tryptic soy agar and on *B. cepacia* selective agar (BCSA) (27) containing 100 μg of trimethoprim/ml. The CFU were counted and bacteria collected for further analysis following incubation at 37°C overnight.

CI. To determine the competitive index (CI) of selected STM mutants, mutant and wild-type bacteria were grown overnight and adjusted to the same optical density at 600 nm. Agar beads prepared from a mixture of parent and mutant combined to give approximately equal numbers (5×10^5 CFU of each strain) were used to inoculate groups of five rats. The ratio of mutant to wild-type bacteria in the inoculum was verified by plating agar beads containing bacteria on BCSA medium with and without trimethoprim to determine viable counts. At 10 days postinfection the lungs were removed, homogenized, diluted, and plated in triplicate on BCSA and BCSA containing 100 μg of trimethoprim/ml. The CI was calculated as the mean output ratio of mutant to wild type divided by the input ratio of mutant to wild-type organisms.

Screening of mutants by real-time PCR. Real-time PCR was performed on *B. cenocepacia* transposon mutants recovered from lung homogenates using the Light Cycler (Roche Diagnostics). Chromosomal DNA was extracted from the bacterial pools and used as a template for real-time PCR using a Faststart DNA Master SYBR Green I kit for DNA amplification and detection (Roche Diag-

nostics). The forward primers used are listed in Table 1, and the reverse primer was STM-LC (5′-AAGGGAGAAAGGCGGACAGGTA-3′). The conditions used for real-time PCR to amplify the 342-bp product were as follows: activation for 10 min at 95°C, followed by 35 cycles of 95°C for 15 s, 55°C for 5 s, and 72°C for 11 s. A melting curve was generated by decreasing the temperature to 65°C, followed by a 0.2°C per second increase in the temperature up to 95°C. Quantitation curves and melting curves were generated for each 35-sample PCR run and analyzed using the Light Cycler software version 3.5 (Roche Diagnostics). Real-time PCR screening for the second screen was performed exactly the same as for the initial screen.

Identification and analysis of transposon insertion sites. The chromosomal sequences surrounding the transposon insertions were identified using the self-cloning strategy as described previously (18). Briefly, chromosomal DNA from the *B. cenocepacia* transposon mutants that passed through the second screen was isolated and subjected to restriction endonuclease digestion by either SalI or NotI (Roche Diagnostics). The digests were ligated under dilute conditions to favor intramolecular ligations with T4 DNA ligase (Roche Diagnostics) and transformed into competent *E. coli* JM109 (70). Transformants were selected on LB agar supplemented with trimethoprim (50 μg/ml). Plasmid DNA was isolated using a High Pure plasmid isolation kit (Roche Diagnostics) and sequenced at the Core Molecular Biology Facility (York University, Ontario, Canada) using primers OTp-3′ (5′-TGTGGCTGCACTTGAACG-3′) or pTn*Mod* (5′-TTCCT GGTACCGTCGACA-3′). The sequences obtained were compared to the Gen-Bank database by BLAST to identify homologous sequences and to data from the *B. cenocepacia* sequencing group at the Sanger Institute for *B. cenocepacia* strain J2315 (http://www.sanger.ac.uk/Projects/B_cenocepacia/).

Analysis of *B. cenocepacia* proteins by two-dimensional gel electrophoresis. Cytosolic proteins were obtained for two-dimensional gel electrophoresis by two passages in a French press (American Instrument Co., Inc., Silver Spring, Md.) at 20,000 lb/in², and the protein concentration was estimated by Bradford assays (4) using Bio-Rad protein assay dye reagent concentrate. Protein from cell lysates (300 μg) was precipitated with 10% trichloroacetic acid, and the pellet was washed first with 5% trichloroacetic acid and then with acetone (25). Precipitated proteins were then subjected to rehydration on Immobiline DryStrip (pH 3 to 10, 13 cm; Amersham Biosciences, Uppsala, Sweden) for 10 h in rehydration solution (8 M urea, 2% 3-[(3-cholamidopropyl)-dimethylammonio]-1-propanesulfonate [CHAPS] and IPG buffer [Amersham Biosciences], pH 3 to 10) containing dithiothreitol, followed by isoelectric focusing for 1 h at 500 V, 1 h at 1,000 V, 5 h at 5,000 V, and 6.25 h at 8,000 V (IPGphor; Amersham Biosciences). After isoelectric focusing, IPG strips were equilibrated in equilibration buffer (50 mM Tris-HCl, pH 8.8, 6 M urea, 30% (vol/vol) glycerol, 2% (wt/vol) SDS, trace bromophenol blue) and applied to a 1-mm thick 12.5% polyacrylamide gel to resolve the second dimension. The gel was overlaid with 0.125% (wt/vol) agarose in SDS electrophoresis buffer containing bromophenol blue (3.02 g of Tris base/liter, 14.42 g of glycine/liter, 1% (wt/vol) SDS in distilled water). Gels were run at 10 mA per gel for 15 min followed by 20 mA for 5 h in SDS electrophoresis buffer. Proteins were visualized by SYPRO orange (Bio-Rad Laboratories) according to the manufacturer's instructions and stained with Coomassie brilliant blue (0.25% Coomassie brilliant blue, 45% methanol, 10% glacial acetic acid; distained with 45% methanol and 10% glacial acetic acid). Gels were dried using a Bio-Rad gel dryer model 583 (Bio-Rad Laboratories). To assess reproducibility and standardize the preparation of extracts and the conditions for running the two-dimensional gel electrophoresis, gels with samples from the wild-type strain K56-2 were run four times, and those with samples from the mutants strains were run twice. Spots were analyzed using ImageMaster 2D Elite software (NonLinear Dynamics, Durham, N.C.).

RESULTS AND DISCUSSION

Construction and characterization of the tag*n* plasposon derivatives. To distinguish individual transposon mutants within a pool, 41 oligonucleotide tags, each consisting of 21 bp, were incorporated into the transposon backbone of pTn*Mod*-OTp′ near one of the inverted repeats to generate 41 unique plasposons pTn*Mod*-OTp′-tag*n* (Fig. 1). The 21-bp oligonucleotides were designed such that the 14 residues at the 5′ end were identical, while the 7-bp region near the 3′ end was unique to each tag (Table 1) (39). The pTn*Mod*-OTp′ plasposon was previously shown to successfully integrate at random into the chromosome of *B. cepacia* complex isolates following

mobilization from an *E. coli* host strain (18–20). The presence of a *dhfr* gene within the transposable element confers resistance to trimethoprim, one of the few antibiotics to which most strains of the *B. cepacia* complex are sensitive (38, 49). Prior to the construction of the transposon mutant library for infection in the animal model, we examined each of the 41 plasposons by PCR to investigate possible cross-amplification among the individual tags. This control was necessary since cross-amplifications would be detrimental to the STM experiment, as potential mutants unable to survive in the in vivo animal model would be misidentified. We tested each of the 41 pTn*Mod*-OTp-tag*n* plasmids against each other using a primer set consisting of an upstream primer that anneals 811 bp upstream of the 21-bp oligonucleotide tag within the transposon (STM-common) and a downstream primer which was the 21-bp oligonucleotide tag itself (Fig. 1). Figure 2A shows a representative gel in which the PCR was performed with the tag2-specific and STM-common primers, with the various pTn*Mod*-OTp-tag*n* plasmids as DNA templates. The absence of PCR amplification in the reactions with all the plasposons not containing tag2 indicated that this tag did not cross-amplify with any of the other tag oligonucleotides. A series of PCRs was performed for each tag primer in a similar manner as with tag2. These experiments allowed us to eliminate four pTn*Mod*-OTp-tag*n* plasposons carrying the oligonucleotide tags 13, 21, 24, and 30, which cross-amplified with other tags (Table 1 and data not shown). The tags in the remaining 37 pTn*Mod*-OTp-tag*n* plasposons did not cross-amplify during PCR amplifications and were thus used for further steps in the STM procedure.

An additional control was done to ensure that the oligonucleotide tags could be detected once the transposon was inserted in the *B. cenocepacia* chromosome. Because the genome of *B. cenocepacia* has an approximate G+C content of 67 mol%, PCR using chromosomal DNA as a template can often yield no amplification products or several nonspecific bands, possibly due to mispriming. In addition, high stringency conditions are required for the PCR amplifications due to the high sequence similarity between the oligonucleotide tags. PCR was performed using the STM-common and tag-specific primers to demonstrate, as shown in Fig. 2B, that the appropriate tag could be detected from *B. cenocepacia* chromosomal DNA. Furthermore, specific tags could also be detected when DNA from mixed cultures was used as a template (Fig. 2B). These preliminary tests demonstrated that the tags and plasposon constructed could be used for the STM screening in *B. cenocepacia*.

Identification of survival-defective mutants by real-time PCR screening. The 37 plasposons were then separately mobilized into *B. cenocepacia* K56-2 by triparental conjugation to produce 96 transposon mutants for each of the tags. The 37 banks of *B. cenocepacia* transposon mutants were next arranged into pools such that any individual pool contained one of each of the tag-specific transposon mutants. Thus, each pool contained 37 distinct transposon mutants which could be individually distinguished from one another by the presence of the unique 21-bp oligonucleotide tag within the integrated transposon. The pools of transposon mutants were separately incorporated into agar beads, and the beads were used for intratracheal lung infection in rats. Each infection was performed in duplicate and allowed to proceed for 10 days, an
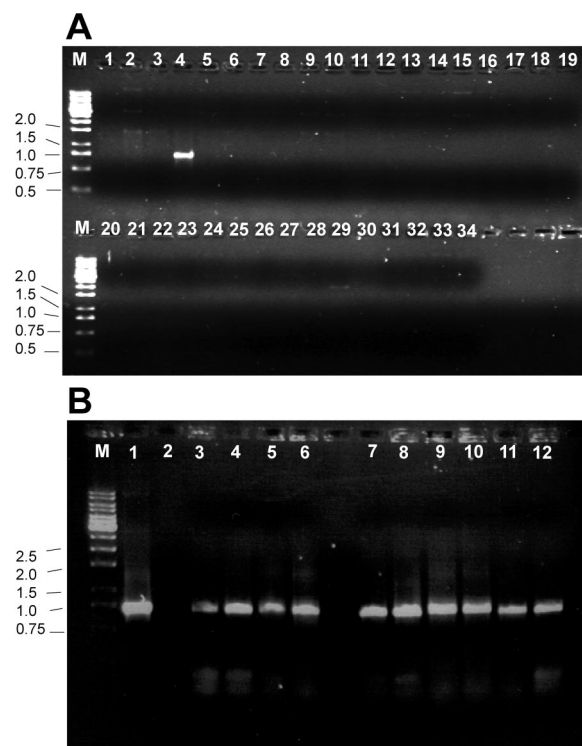

FIG. 2. Representative gels of control experiments testing specificity of the tags and sensitivity of the PCR amplification to detect the tags on the chromosome. (A) The tag2 plasposon does not cross-amplify with the other tag oligonucleotides. PCR was performed using the plasposon pTn*Mod*-OTp-tag2 as a template. The primer STM-common was used with a different tag-specific primer in each reaction. Lane M: 1-kb ladder molecular weight markers; lane 1, distilled H_2O template with tag2 primer (reaction negative control); lane 2, pTn*Mod*-OTp′ lacking tag insertions with tag2 primer (template negative control). Lanes 3 to 34 were loaded with amplification products from the reactions containing pTn*Mod*-OTp-tag2 template and each of the various tag*n* primers, beginning with lane 3 using tag1 until lane 34 using tag32. PCR amplification is specific for tag2 as indicated by the lack of PCR amplification in all lanes except lane 4. (B) Tag oligonucleotides can be detected from the *B. cepacia* chromosome by PCR after transposition. For each PCR amplification, the primer STM-common was used in combination with the indicated tag*n*-specific primer. Lane M: 1-kb ladder molecular weight markers; lane 1, pTn*Mod*-OTp-tag1 with the tag1 primer (template positive control); lane 2, pTn*Mod*-OTp′ with the tag1 primer (template negative control); lanes 3 to 6, PCR amplifications with the tag1 primer using chromosomal DNA from four independent K56-2::tag1 transposon mutants; lanes 7 to 10, PCR amplifications with the tag2 primer using chromosomal DNA from four independent K56-2::tag2 transposon mutants; lanes 11 and 12, PCR amplifications with the tag1 (lane 11) and tag2 (lane 12) primers using chromosomal DNA from a mixed culture containing K56-2::tag1 and K56-2::tag2 mutants.

interval which results in chronic lung infection (C. Kooi and P. A. Sokol, unpublished data). After the 10-day infection, the lungs were removed and the recovered bacteria were collected for DNA preparation and PCR screening to identify the surviving mutants in each original pool.

The 21-bp oligonucleotide tags containing unique sequences within each transposon enabled differentiation of mutants that were present from those mutants which were absent from each of the output pools. DNA from the *B. cenocepacia* mutants that were recovered from the lung infections served as tem-

plates for PCR amplification. Because infections with each pool of mutants were carried out in duplicate, screening of mutants was done with the infection that exhibited the highest bacterial yield, as this would result in the lowest probability of false negatives. We used real-time PCR amplification with primer sets similar to those employed to test cross-reactivity (STM-LC and each specific tag oligonucleotide). Quantitation and melting curves were generated for each of the PCR amplifications. Figure 3 illustrates the data analysis of one PCR run. For each run, a positive and a negative control were included together with 33 sample reactions. The product quantitation curve (Fig. 3A) indicated the amount of double-stranded PCR product generated following each cycle. In the case of DNA prepared from bacteria recovered from rat lungs, we observed quantitation curves ranging from no product to more product than with the positive control. After each round of PCR amplification, a melting curve was generated for each run of 35 samples (Fig. 3B). This demonstrated whether a PCR product generated was specific, by comparing it with the product from the positive control reaction, which consistently had a peak at about 88°C. The melting curve was more informative than the quantitation curve because it indicated whether or not the observed amplification was specific. Figure 3C shows a subset of the melting curves in Fig. 3B, including the positive and negative control plus three sample reactions. In this example, the tag7 mutant in pools F4b and H8b did not amplify with the tag7-specific primer, and therefore these mutants were not present in the pool and would pass through this screening procedure. Seventy-one pools of *B. cenocepacia* transposon mutant chromosomes were screened in this manner with the 37 tag primers. One important limitation of STM for in vivo screening is that the inoculated pool must have a dose such that each mutant is well represented and is able to establish an infection. To determine if this was the case with our pools, the input pools were randomly examined by real-time PCR, and the amplified DNA from the mutants in these pools gave similar quantitation curves, suggesting that the individual mutants were present at similar concentrations (data not shown). Mutants attenuated for survival in the animal model were scored as those whose genomic DNA did not reveal any PCR amplification after 28 cycles on the quantitation curve or, alternatively, had low or nonspecific melting peaks (peaks not at about 88°C) on the melting curve. According to these criteria, 260 of the 2,627 mutants that we assayed were putatively identified as having a survival defect in the animal model.

To eliminate potential false positives due to the large number of mutants in each pool, the 260 mutants obtained from the first screen were rearranged into 30 smaller pools containing 6 to 13 mutants per pool. Each pool was encased into agar beads and used to infect duplicate rats for 10 days as before. The output pools were reanalyzed by real-time PCR as for the first screen, except that this second screen was much more stringent. Only those mutants that did not show any amplification after 35 cycles in the quantitation curve and had no demonstrable peak in the melting curve were considered to pass this second screen. After the second screen, 102 mutants were identified, each containing transposon insertions in candidate genes required for the survival of *B. cenocepacia* in the rat agar bead model. Our finding that 102 out of 2,627 mutants (3.8%) were unable to survive in an in vivo model correlated well with
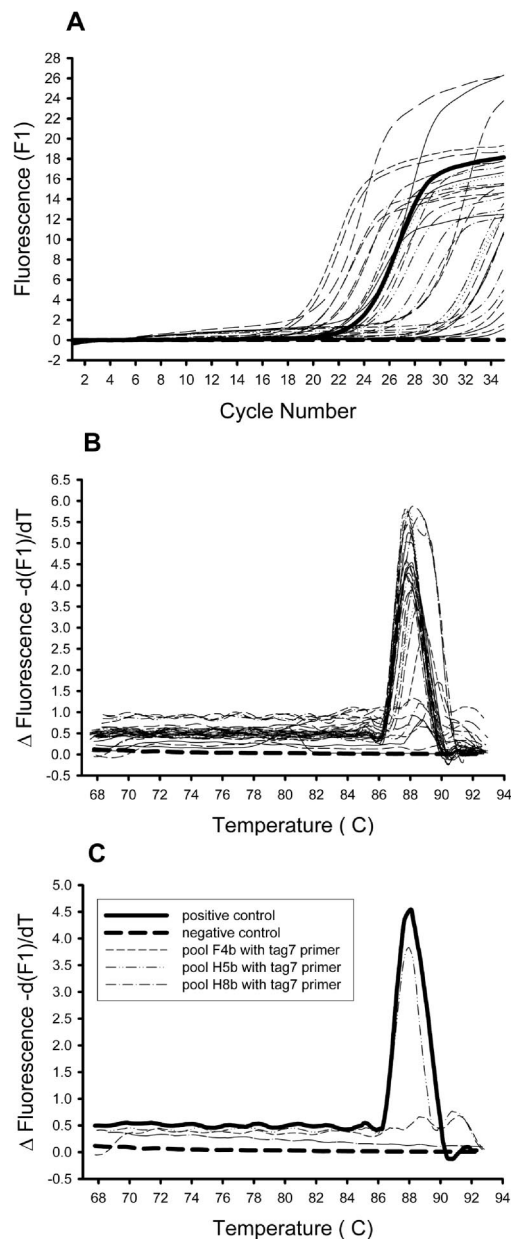

FIG. 3. Sample real-time PCR results from the STM screen. An example of one run of 35 samples is shown with 33 output pools plus a positive and negative control sample. (A) Quantitative curve showing the PCR amplification (measured as relative fluorescence units) in real time after each cycle. (B) Melting curve showing the change in fluorescence as the temperature is increased from 68 to 94°C. The specific PCR product can be seen as a sharp peak at approximately 88°C. For panels A and B, the positive control is shown as a thick solid line and the negative control as a thick dashed line. (C) A subset of the PCR amplifications shown in panels A and B were taken, and a melting curve was generated. The positive and negative controls are shown along with three representative output pools. The melting curve of pool H5b is similar to the positive control and therefore does not contain a mutant important for survival in vivo. The melting curves of pools F4b and H8b indicate no PCR amplification, and therefore the mutants are not in the pools and contain transposon insertions in genes important for survival in the animal model.
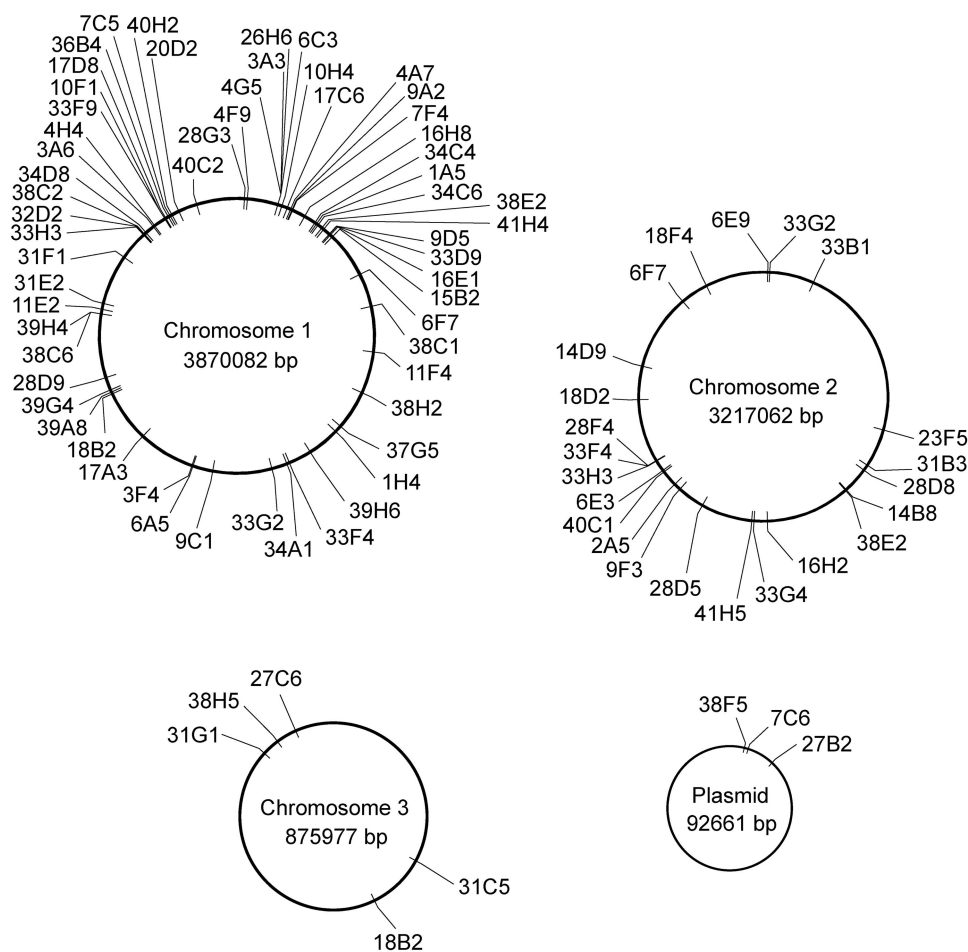
FIG. 4. Schematic representation of the chromosomal locations of the transposon insertions of *B. cenocepacia* K56-2 survival-defective mutants. This genome map is based on sequence information generated for *B. cenocepacia* strain J2315 by the *B. cepacia* Sequencing Group at the Sanger Institute and can be obtained at http://www.sanger.ac.uk/Projects/B_cepacia.

figures obtained from previous STM experiments using other bacterial pathogens, which have detected a frequency of survival-defective mutants ranging from 0.2 to 13% (48). The survival-defective mutants did not appear to have growth defects in vitro, as all of them grew in nutrient broth at levels comparable with the wild-type K56-2 (data not shown).

Identification of genes required for survival in vivo and confirmation of the predictive value of the STM screen. The nucleotide sequence of the DNA flanking the site of transposon insertion obtained for each of the 102 attenuated mutants was used to search the GenBank databases for homologous genes. The results of this analysis are shown in Table 2, with the genes assigned to one of five functional categories: metabolism, DNA replication/recombination/translation, regulation, cell surface, and transport. Insertions in genes encoding proteins with no significant homology to proteins in the databases or homologous to proteins or predicted proteins of unknown function were categorized as unknown. Whenever possible, insertions were mapped to the three chromosomes and large plasmid of strain J2315 (Fig. 4), whose genome has been entirely sequenced (http://www.sanger.ac.uk/Projects/B_cepacia/). *B. cenocepacia* strains J2315 and K56-2 belong to the same clonal

group, and their genomes share similar macrorestriction patterns (43). Ninety-eight of the K56-2 mutants contained a single transposon insertion, while four mutants had two insertions located on different chromosomes. Previous mutagenesis experiments in a *Burkholderia vietnamiensis* strain with various plasposons also revealed, in some cases, mutants with several transposon insertions in different locations (C. Fehlner-Gardiner and M. A. Valvano, unpublished observations). Fifty-seven of the 102 insertions mapped to chromosome 1, 22 insertions mapped to chromosome 2, five insertions were located on chromosome 3, and three insertions were found in the 90-kb plasmid (Fig. 4). In most cases, the DNA sequence obtained from the regions flanking the insertions in K56-2 was nearly identical (90 to 100% identity) to the J2315 sequence (Table 2). However, the DNA sequence of regions near the transposon insertion in mutants 17D8, 33G2, 40H2, and 6C3 showed a lower level of identity with J2315 counterparts that ranged from 68 to 88%, indicating that at least in these regions there may be more variability between strains K56-2 and J2315. Despite the fact that both K56-2 and J2315 are clonal, their genomes are not completely identical (43); therefore, it is possible that the insertions with lower identity to genes in

TABLE 2. Identification of the genes with transposon insertions in the survival-defective mutants of *B. cenocepacia* K56-2

Class	Mutant	Location or similarity [gene (species); accession no.][a]	Known or putative function[f]	Type of insertion[b]	Location in J2315	% DNA identity to J2315
Metabolism	1A5	RSp0749 (*Ralstonia solanacearum*); NP_522310	ClpA, chaperone, ATPase	INT	Chromosome 1	100
	2A5	Rsc0772 (*Ralstonia solanacearum*); NP_518893	Cytochrome c (oxidoreductase/dehydrogenase)	CDS	Chromosome 2	99
	3F4	Bcep0615 (*Burkholderia* sp.)[c]; ZP_00027845	Phosphate starvation-inducible protein	CDS	Chromosome 1	94
	3A6	Bcep4150 (*Burkholderia* sp.)[c]; ZP_00031317	xdhA, xanthine dehydrogenase subunit A	CDS	Chromosome 1	99
	4A7	Bcep0315 (*Burkholderia* sp.)[c]; ZP_00027557	paaE, ferredoxin reductase	CDS	Chromosome 1	100
	4F9	Bcep0165 (*Burkholderia* sp.)[c]; ZP_00027409	Long-chain fatty acid CoA ligase	CDS	Chromosome 1	94
	6E9	Bcep1341 (*Burkholderia* sp.)[c]; ZP_00028560	tdh, Zn^{2+}-dependent threonine-3-dehydrogenase	CDS	Chromosome 2	77
	9F3	blr0281 (*Bradyrhizobium japonicum*); BAC455546	oxd, oxalate decarboxylase	CDS	Chromosome 2	99
	17D8	CAC3312 (*Clostridium acetobutylicum*); NP_349904	fkbH, methoxymalonyl-ACP biosynthesis	UP	Chromosome 1	83
	18D2	Bcep7606 (*Burkholderia* sp.)[c]; ZP_00034711	Succinyl-diamino-pimelate desuccinylase	CDS	Chromosome 2	99
	20D2	Bcep3497 (*Burkholderia* sp.)[c]; ZP_00030674	D-lactate-dehydrogenase/oxidoreductase	INT	Chromosome 1	98
	28D9	Bcep033 (*Burkholderia* sp.)[c]; ZP_00027284	Translation initiation inhibitor, TdcF and yjgF family and just upstream from phenazine biosynthesis protein (epimerase)	CDS	Chromosome 1	98
	31C5	Chlo1457 (*Chloroflexus aurantiacus*); ZP_00018467	Acetyltransferase of the GNAT family	CDS	Chromosome 3	99
	31F1	Bcep5460 (*Burkholderia* sp.)[c]; ZP_00032601	xdhC, xanthine dehydrogenase chaperone	UP	Chromosome 1	100
	31E2	Bcep2710 (*Burkholderia* sp.)[c]; ZP_00029902	amiC, N-acetyl-muramoyl-L-alanine-amidase	CDS	Chromosome 1	97
	33G2[d]	Bcep4417 (*Burkholderia* sp.)[c]; ZP_00031577	Enoyl-CoA hydratase	CDS	Chromosome 1	88
	33G4	Reut3200 (*Ralstonia metallidurans*); ZP_00024228	tyrB, aromatic amino acid transferase	CDS	Chromosome 2	95
	38E2[d]	Bcep3466 (*Burkholderia* sp.)[c]; ZP_00030645	hemK, methyl transferase	CDS	Chromosome 1	99
	39H6	Rscl246 (*Ralstonia solanacearum*); NP_519367	iolG, myo-inositol 2-dehydrogenase	CDS	Chromosome 1	100
	39A8	Bcep0325 (*Burkholderia* sp.)[c]; ZP_00027566	NADPH quinone oxidoreductase	CDS	Chromosome 1	99
	40C2	Bcep6429 (*Burkholderia* sp.)[c]; ZP_00033555	glk, gluconate kinase 2 (thermoresistant)	CDS	Chromosome 1	99
DNA repair/replication/translation	7C6	Bb3088 (*Bordetella bronchiseptica*); NP_889624	dnaE, DNA polymerase III alpha chain	CDS	Plasmid	99
	7F4	BVI17805 (*Burkholderia vietnamiensis*); Y18705	23S rRNA gene	CDS	Chromosome 1	100
	9A2	BVI17805 (*Burkholderia vietnamiensis*); Y18705	23S rRNA gene	CDS	Chromosome 1	100
	9D5	PC23RRNA (*Burkholderia cepacia*); X16368	23S rRNA gene	CDS	Chromosome 1	100
	33D9	PC23RRNA (*Burkholderia cepacia*); X16368	23S rRNA gene	CDS	Chromosome 1	100
	11F4	XAC1107 (*Xanthomonas axonopodis*); NP_641445	Integrase/resolvase/recombinase	CDS	Chromosome 1	96
	15B2	RSc3441 (*Ralstonia solanacearum*); NP_521560	dnaN, DNA polymerase III beta chain	UP	Chromosome 1	92
	16E1	hsdM1 (*Chlorobium tepidum*); NP_661571	Type I restriction system adenine methylase	INT	Chromosome 1	99
	27B2	retA (*Serratia marcescens* incL/M plasmid R471a); AAC82519	Reverse transcriptase	CDS	Plasmid	96
	27C6	PCRRN5S (*Burkholderia cepacia*); X02629	5S rRNA gene	CDS	Chromosome 3	95
	28F4	repA (*Pseudomonas fluorescens* pAM10.6 plasmid); AAG23805	Replication protein	UP	Chromosome 2	98
	28G3	Bcep2527 (*Burkholderia* sp.)[c]; ZP_00029720	gidA, glucose-inhibited protein division A	CDS	Chromosome 1	100
	31B3	DNA methylase (*Burkholderia multivorans*); BAC65265	DNA methyl-transferase	CDS	Chromosome 2	99
	40C1	Bcep6969 (*Burkholderia* sp.)[c]; ZP_00034082	Phosphoesterase; DNA repair exonuclease	CDS	Chromosome 2	96

Category	Clone	Homolog (organism); accession	Description	Type	Location	%
Regulatory	1H4	*nasR* (*Klebsiella oxytoca*); Q48468	Nitrate/nitrite response regulator	UP	Chromosome 1	99
	4G5	*hns* (*Ralstonia solanacearum*); NP_591826	H-NS transcriptional regulator (histone family)	CDS	Chromosome 1	99
	4H4	Bcep6214 (*Burkholderia* sp.); ZP_00033342	LysR family of transcriptional regulators	CDS	Chromosome 1	97
	14B8	Bcep5162 (*Burkholderia* sp.); ZP_00032313	LysR family of transcriptional regulators	UP	Chromosome 2	98
	11E2	Bcep2955 (*Burkholderia* sp.)[c]; ZP_00030142	Sensory protein with Rtn domain	UP	Chromosome 1	99
	18B2[d]	Bcep2486 (*Burkholderia* sp.)[c]; ZP_00029679	OmpR family response regulator	CDS	Chromosome 1	96
	34A1	Bcep4207 (*Burkholderia* sp.)[c]; ZP_00031373	Transcriptional regulator, sigma factor 54	CDS	Chromosome 1	98
	38C6	Bcep8011 (*Burkholderia* sp.); ZP_00035109	*cspC*, cold shock protein transcriptional regulator	CDS	Chromosome 1	90
	39H4	Bcep8011 (*Burkholderia* sp.)[c]; ZP_00035109	*cspC*, cold shock protein transcriptional regulator	CDS	Chromosome 1	90
	40H2	*tetR* (*Salmonella enteritidis*); AAN40999	Tetracycline resistance repressor	CDS	Chromosome 1	75
Cell surface	6A5	Bcep1318 (*Burkholderia* sp.)[c]; ZP_00028537	*arnC*; polymyxin resistance, glycosyl transferase	CDS	Chromosome 1	98
	7C5	*yggB* (*Burkholderia mallei*); AAK26451	Small-conductance mechanosensitive channel	CDS	Chromosome 1	99
	28D8	*galU* (*Burkholderia pseudomallei*); AAG24457	UTP-glucose-1-phosphate uridylyltransferase	UP	Chromosome 2	92
	32D2	*wbiF* (*Burkholderia mallei*); AAK27402	Glycosyltransferase, LPS synthesis	CDS	Chromosome 1	91
	33H3[d]	*wbiI* (*Burkholderia mallei*); AAK27405	Epimerase/dehydratase, LPS synthesis	CDS	Chromosome 1	99
	34C6	RS01942 (*Ralstonia solanacearum*); NP_522327	Transmembrane protein, cell wall biogenesis	CDS	Chromosome 1	99
	34D8	*rmlD* (*Burkholderia mallei*); AAK27394	dTDP-4-keto-L-rhamnose reductase, LPS synthesis	CDS	Chromosome 1	99
	36B4	*cpxA* (*Neisseria meningitidis*); NP_283042	Capsule polysaccharide export ATP-binding protein	CDS	Chromosome 1	99
	38C2	SYNW0645 (*Synechococcus* sp.); NP_896738	Glycosyltransferase, LPS synthesis	CDS	Chromosome 1	99
	41H5	Bcep6693 (*Burkholderia* sp.)[c]; ZP_00033811	*pbp1*, penicillin binding protein (cell wall synthesis)	CDS	Chromosome 2	99
Transport	3A3	CV1105 (*Chromobacterium violaceum*); NP_900675	Cation efflux protein	UP	Chromosome 1	96
	26H6	CV1105 (*Chromobacterium violaceum*); NP_900675	Cation efflux protein	UP	Chromosome 1	99
	6C3	Bcep6477 (*Burkholderia* sp.)[c]; ZP_00033603	Permease, major facilitator superfamily	UP	Chromosome 1	68
	6E3	Bcep6966 (*Burkholderia* sp.)[c]; ZP_00034080	*mgtC*, magnesium transport ATPase protein	CDS	Chromosome 2	94
	6F7	Bcep4313 (*Burkholderia* sp.)[c]; ZP_00031476	Na$^+$-dependent transporter	UP	Chromosome 2	98
	14D9	YPO2237 (*Yersinia pestis*); NP_405778	*uhpC*, sugar phosphate permease	CDS	Chromosome 2	98
	16H2	BPP0439 (*Bordetella parapertussis*); NP_882791	Potassium channel protein	UP	Chromosome 2	98
	16H8	Bcep3454 (*Burkholderia* sp.)[c]; ZP_00030633	*ugpB*, glycerol-3-P binding periplasmic protein	CDS	Chromosome 1	94
	18F4	RS03722 (*Ralstonia solanacearum*); NP_521805	Outer membrane hemin binding receptor	UP	Chromosome 2	94
	28D5	Bcep1249 (*Burkholderia* sp.)[c]; ZP_00028468	Low-pH inducible transmembrane protein	CDS	Chromosome 2	98
	33B1	Reut5126 (*Ralstonia metallidurans*); ZP_00026117	Mechanosensitive ion channel	CDS	Chromosome 2	93
	38C1	Reut0257 (*Ralstonia metallidurans*); ZP_00021356	ABC transporter transmembrane permease	CDS	Chromosome 1	97
	38E2[d]	PP3940 (*Pseudomonas putida*); NP_746070	*uhpC*, sugar phosphate permease	CDS	Chromosome 2	95
	41H4	*oxlT2* (*Archaeoglobus fulgidus*); NP_069203	Oxalate/formate antiporter	CDS	Chromosome 1	96

TABLE 2—Continued

Class	Mutant	Location or similarity [gene (species); accession no.]^a	Known or putative function^f	Type of insertion^b	Location in J2315	% DNA identity to J2315
Unknown	9C1	Bcep1803 (*Burkholderia* sp.)^c; ZP_00029009	Hypothetical protein	CDS	Chromosome 1	98
	10F1	jhp0052 (*Helicobacter pylori*); NP_222774	Hypothetical protein (same gene as in 33F9)	UP	Chromosome 1	98
	10H4	CAC2823 (*Clostridium acetobutylicum*; AAK80767	Conserved protein	CDS	Chromosome 1	99
	17A3	Bcep4709 (*Burkholderia* sp.)^c; ZP—0031868	Hypothetical protein	DS	Chromosome 1	90
	17C6	Bcep1157 (*Burkholderia* sp.)^c; ZP—00028378	Hypothetical protein	UP	Chromosome 1	96
	18B2^d	No matches in databases	Hypothetical protein	CDS	Chromosome 3	92
	23F5	Bcep0344 (*Burkholderia* sp.)^c; ZP_00027585	Hypothetical protein	UP	Chromosome 2	99
	31G1	Bcep2682 (*Burkholderia* sp.)^c; ZP_00029874	Hypothetical protein	CDS	Chromosome 3	98
	33G2^d	Bcep5345 (*Burkholderia* sp.)^c; ZP_00032488	Conserved hypothetical protein	CDS	Chromosome 2	94
	33H3^d	No matches in databases	Hypothetical protein	CDS	Chromosome 2	99
	33F4	Bcep6478 (*Burkholderia* sp.)^c; ZP_00033604	Hypothetical protein; lipoprotein?	UP	Chromosome 1	99
	33F9	jhp0052 (*Helicobacter pylori*); NP_222774	Hypothetical protein (same gene as in 10F1)	UP	Chromosome 1	94
	34C4	RSp0741 (*Ralstonia solanacearum*); NP_522302	Hypothetical transmembrane protein	UP	Chromosome 1	92
	37G5	RSp0747 (*Ralstonia solanacearum*); NP_522308	Conserved bacterial protein	INT	Chromosome 1	99
	38H2	*yftI* (*Escherichia coli* CFTG073); AAN82100	Hypothetical protein	CDS	Chromosome 1	99
	38F5	Just downstream of replication protein gene *trfA*	Putative plasmid replication *ori*		Plasmid	99
	38H5	Unknown, not near any predicted open reading frames			Chromosome 3	
	39G4	PP2099 (*Pseudomonas putida*); NP_744249	Conserved bacterial protein	INT	Chromosome 1	
Undetermined^c	4A6	Unknown location		INT		
	20C7	Unknown location; near an IS*407* insertion		INT		
	20E9	Unknown location		INT		
	20H6	Unknown location; near an IS*407* insertion		INT		
	23G8	Unknown location		INT		
	25A3	Unknown location; near 23S rRNA cluster and IS*407*		INT		
	33B4	Unknown location; near 5S rRNA cluster		INT		
	36C2	Unknown location; near 5S rRNA cluster		INT		
	37A8	Unknown location		INT		
	37E1	Unknown location; near an IS*407* insert		INT		
	37H8	Unknown location		INT		
	38F4	Unknown location; near 23S rRNA cluster and IS*407*		INT		
	39C9	Unknown location		INT		
	39D7	Unknown location		INT		
	39D8	Unknown location		INT		
	41A6	Unknown location; near 23S rRNA cluster and IS*407*		INT		
	41C6	Unknown location; near 5S rRNA cluster		INT		
	41C9	Unknown location		INT		
	41F7	Unknown location; near 23S rRNA cluster and IS*407*		INT		

^a Sequenced gene in public databases with the highest similarity to STM sequences. Names of source bacteria are shown in parentheses. In some instances, gene designations are from whole genome sequences, giving a two-letter code for the bacterium followed by the sequence number (e.g., NP_522310).
^b UP, transposon insertion upstream of gene (possibly within promoter region); CDS, transposon insertion within coding region; INT, entire plasposon integrated in the K56-2 chromosome or plasmid.
^c This isolate is erroneously designated in the databases as *B. fungorum* strain LB400.
^d Two insertions in different locations were found in the same mutant strain.
^e These mutants have all of the entire plasposon integrated into the genome of *B. cenocepacia* K56-2, but the precise location of the integration could not be determined.
^f ACP, acyl carrier protein; LPS, lipopolysaccharide.

TABLE 3. Competition assays of selected mutants
identified by STM

Mutant	Gene or putative function[a]	CI[b]
28D5	Low-pH inducible transmembrane protein	0.009
4A7	*paaE*, ferredoxin reductase	0.040
7D8	*fkbH*, methoxymalonyl-ACP biosynthesis, capsule biosynthesis?	0.001
36B4	*cpxA*, capsule export	0.069
18F4	Outer membrane hemin binding receptor	0.034
10F1	Hypothetical protein	0.109
3A6	*xdhA*, xanthine dehydrogenase	0.001
4F9	Long-chain fatty acid CoA ligase	0.028
6A5	*arnC*(*pmrF*), glycosyltransferase involved in the biosynthesis of aminoarabinose	0.063
28D8	*galU*, UTP-glucose-1-phosphate uridylyltransferase	0.007
33H3	*wbiI*, epimerase/dehydratase, LPS synthesis	0.034
6E3	*mgtC*, magnesium transport ATPase protein	0.006

[a] ACP, acyl carrier protein; LPS, lipopolysaccharide.
[b] The CI is defined as the mean output ratio (mutant/wild type) divided by the input ratio (mutant/wild type) from groups of five rats infected with approximately 5×10^5 CFU of each strain embedded in agar beads.

J2315 may be located on regions of higher genetic variation between the two strains. Twenty mutants contained insertions in chromosomal regions between open reading frames (Table 2), which are presumably affecting the promoter of the gene or gene clusters located downstream from the insertion site. Twenty-four mutants had the entire plasposon integrated in the chromosome, and the location of the integration was mapped in five of them. The precise location of the insertion in the remaining 19 mutants could not be determined, because the endpoints of the plasposon insertion were within the repeated element IS*407* or an rRNA cluster. Since there are six homologous rRNA gene clusters on the J2315 genome and up to 14 copies of IS*407*, we could not establish unequivocally the exact location of the transposon insertion in these mutants. These regions may represent hot spots for recombination, probably due to homologies with short sequences within the Tn*5* transposase gene of the plasposon.

To verify the predictive value of our STM screen, we determined the CI of individual mutants, by infecting rats with beads prepared from a mixture of wild-type and mutant bacteria. Because of the large number of attenuated mutants identified in this study, we selected 12 individual mutants representing the various groups of affected genes. The results in Table 3 show that the individual mutants displayed various levels of attenuation with CI values ranging from 0.001 to 0.109. Only one mutant, 10F1, with an insertion within an unknown gene encoding a hypothetical protein showed less than a 1-log difference in survival with respect to the wild-type K56-2 strain, while the others displayed 2- and 3-log differences (Table 3), indicating that they were attenuated. A considerable amount of variation when mutants are individually tested despite the fact that they are consistently recovered from the mixed pools has been reported in other STM studies (45). These variations may reflect more subtle influences on in vivo bacterial survival that are not seen at higher doses or in less diverse populations. Further in vivo analysis of these and the remaining mutants will help to determine the relative importance of the affected genes in pathogenesis of *B. cenocepacia* infection.

Characterization of the STM mutants. We uncovered mutations in several genes and gene clusters that are involved in cellular metabolism, even though we eliminated auxotrophic mutants prior to the in vivo selection step by recovering transposon mutants on minimal media. Survival-deficient mutants with putative defects in xanthine dehydrogenase, threonine-3-dehydrogenase, oxalate decarboxylase, glycerol-3-phosphate-binding periplasmic transport protein, succinyl-diamino-pimelate desuccinylase, D-lactate dehydrogenase, *N*-acetyl-muramoyl-L-alanine-amidase, enoyl-coenzyme A (CoA) hydratase, aromatic amino acid transferase, and quinone oxidoreductase suggest unique metabolic needs for *B. cenocepacia* in the lungs. This is especially important when taking into account that these mutants appeared to grow in VBM minimal medium at comparable rates relative to the wild-type isolate (data not shown). Similar observations were made in previous STM screens that also resulted in the identification of several metabolic genes (8, 17, 28).

B. cenocepacia genes involved in DNA replication and repair functions, such as those encoding DNA polymerase III alpha and beta chains, type I restriction-modification enzymes, reverse transcriptase, a glucose-inhibited division protein, a DNA methyl-transferase, a replication factor, and a DNA repair exonuclease, were also found in our STM screen. Similar genes were also identified in previous STM screens using other bacteria (14, 45), suggesting that the altered environment encountered by bacteria in vivo may require the intact function of genes involved in DNA modifications. A mutation in a glucose-inhibited division gene that regulates the translation of a cytotoxin in *Aeromonas hydrophila* has recently been reported (58), suggesting that the mutated *B. cenocepacia* gidA could have a similar regulatory role on genes or gene products required for in vivo survival. Three of the survival-defective mutations were located on the plasmid, two of them compromising genes involved in plasmid maintenance and the other located within a putative replication region. We speculate that these insertions may result in the instability of the 90-kb plasmid in vivo. It is possible that the instability or even loss of the plasmid in vivo may impair the survival of the plasmid-free bacterial cells by mechanisms involving killing or growth reduction of these cells (for a recent review, see reference 26). Further research is currently under way in our laboratory to explore this possibility. In addition, four survival-attenuated mutants had insertions within two rRNA clusters. While the role of rRNA clusters in virulence is not known at this time, others have found that five of the seven rRNA operons present in *E. coli* are necessary to support near-optimal growth on complex media, while all seven operons are necessary for rapid adaptation to nutrient and temperature changes (11). Therefore, it is conceivable that a similar situation occurs for *B. cenocepacia*, and adaptation to the environmental conditions found in vivo may require a full complement of rRNA operons.

We detected several mutants with insertions in putative regulatory genes, including members of the LysR family of transcriptional regulators, an H-NS-like protein, a TetR repressor, a regulator from the cold shock family, and two members of the sensor kinase two-component regulatory systems. It is conceivable that the survival-defective phenotype of these mutants may be due to the dysregulation of effector genes whose expression is controlled or modulated by these proteins rather
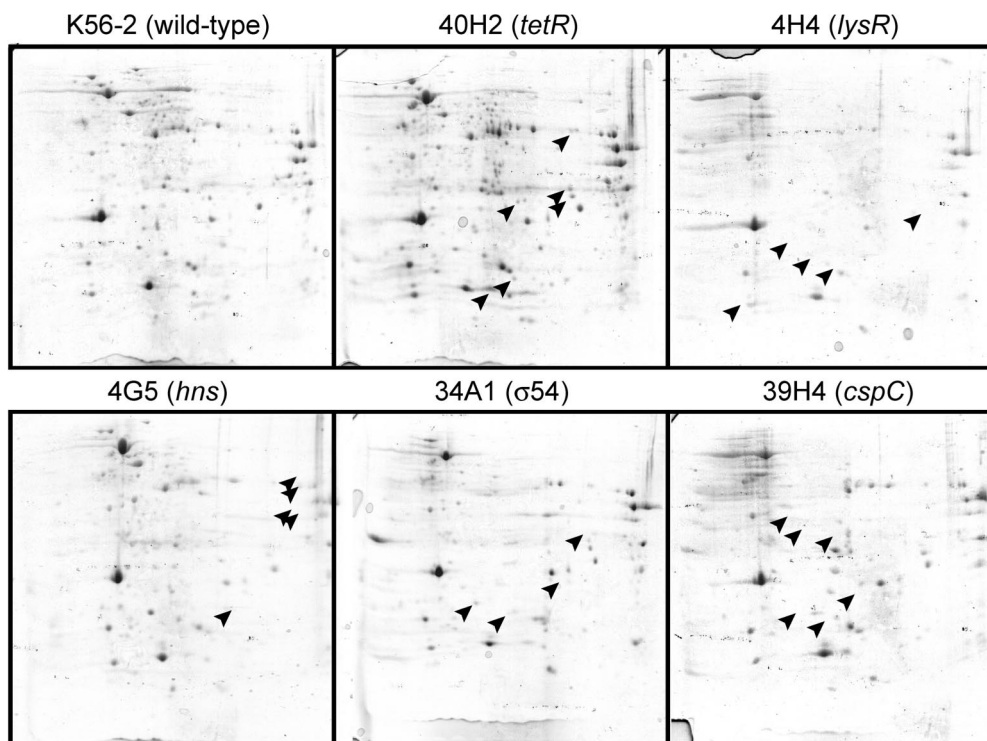
FIG. 5. Two-dimensional gel electrophoresis analysis of the parental *B. cenocepacia* K56-2 (wild type) and STM mutants predicted to contain insertions in regulatory genes (Table 2). Isoelectric focusing from pH 3 to 10 was performed for the first dimension (left to right, horizontal), and SDS-PAGE was performed for the second dimension (vertical) for each gel. Proteins were stained with Coomassie brilliant blue for visualization. Arrowheads in 40H2, which has an insertion in a gene encoding a putative protein repressor of the TetR family, indicate protein spots not present in the wild-type strain K56-2. Arrowheads in the gels from the other mutants indicate the most obvious protein spots that are present in K56-2 but absent in the mutant strains, all of which have insertions in genes encoding putative positive regulators.

than the lack of the regulator itself. To determine whether these regulatory genes indeed encode global regulators, we compared the profiles of cytosolic proteins of each mutant and the K56-2 parental isolate by two-dimensional gel electrophoresis (Fig. 5). The profiles of mutants 4H4 (predicted LysR transcriptional regulator homologue), 4G5 (predicted H-NS regulatory gene), 34A1 (σ^{54} homologue), 38C6 and 39H4 (cold shock family of transcriptional regulator), and 40H2 (Tet-repressor regulator homologue) were compared to that of the wild-type K56-2. The mutant 40H2, containing an insertion in the TetR family repressor homologue, revealed additional protein spots not observed in the parental K56-2 lysate, whereas mutants containing insertions in positive regulators lacked several protein spots that are present in the lysate from the parental K56-2 strain (Fig. 5). These results are consistent with the predicted roles for these regulatory proteins. Ongoing research is underway to confirm that these regulators are indeed involved in the different protein expression profiles observed, to characterize the regulated proteins from the proteome of K56-2, and to determine the components of each regulon.

We found 14 attenuated mutants with insertions compromising genes involved in transport functions, including a cation efflux protein (mutants 3A3 and 26H6), several permeases, and ABC transporters (Table 2). One other insertion was found just upstream of a gene encoding a predicted 96-kDa outer membrane heme-binding receptor protein (mutant 18F4). This is the first gene of a putative operon that may be involved in

heme uptake. Heme-binding proteins of molecular masses ranging from 96 to 100 kDa have been recently described in many strains of the *B. cepacia* complex (60). Expression of heme-binding proteins leading to heme binding and accumulation is associated with virulence in several gram-negative pathogens (36). For example, in *Porphyromonas gingivalis* the accumulation of heme appears to protect bacterial cells against damage from hydrogen peroxide (59). Thus, an outer membrane heme-binding protein may contribute to in vivo survival by enabling *B. cenocepacia* to withstand oxidative stresses in inflammatory exudates in the lung.

Mutant 6E3 has an insertion interrupting a gene that encodes a homologue of the MgtC protein. This protein is required in *S. enterica* and *Mycobacterium tuberculosis* for growth under Mg^{2+}-limiting environments, as well as for survival within macrophages and virulence in vivo (2, 5). Preliminary experiments indicate that, unlike the wild-type strain K56-2, the growth of this mutant is drastically reduced at Mg^{2+} concentrations of 25 μM or lower (K. Maloney and M. A. Valvano, unpublished data). Since *B. cepacia* complex strains can survive intracellularly within amoebae and macrophages (44, 56), we speculate that the MgtC protein homologue may be required for survival in vivo during lung infection in the rat model.

Additional mutants within this category had insertions in genes encoding enzymes required for the synthesis of O-antigen LPS (mutants 32D2, 33H3, 34D8, and 38C2). The isolation

of genes involved in LPS synthesis for survival in vivo is not unexpected, as nearly all STM studies of gram-negative pathogens have reported similar findings (8, 17, 28, 33, 63). The detailed characterization of the O-antigen LPS biosynthesis cluster in K56-2 and J2315 strains will be described in detail elsewhere (X. Ortega, T. A. Hunt, and M. A. Valvano, manuscript in preparation).

Conclusion. The majority of the genes identified in our STM screen do not correspond to classical virulence factors proposed by others for *B. cenocepacia*. Given the large size of the *B. cenocepacia* genome (8.056 Mbp), it is possible that our screen has not uncovered all the genes required for in vivo survival. Also, it is important to point out that our screen was specifically designed to detect factors involved with in vivo survival and persistence in the lungs from our rat model. Early colonization steps are bypassed in our lung infection model, as bacteria instilled intratracheally are previously encased in agar beads. Thus, we did not expect to find mutants in genes involved with mucosal colonization. Also, STM screens do not usually detect extracellular factors that may be required for infection, since these factors may be provided by other mutants in the pool. The real-time PCR screening described in this study greatly reduced the time required for the screening step while increasing the sensitivity and specificity by allowing quantification of the PCR products produced. In addition, the plasposons and the bank of transposon mutants we generated will permit us to screen for bacterial genes required for survival in other in vivo models. An important limitation of STM screens is that the insertions may cause polar effects on the expression of downstream genes, which is especially true for those insertions in genes that are part of operons and those located upstream of coding regions, which may affect promoter elements or other regulatory elements. Therefore, our results should not be overinterpreted, as they provide a list of genes that are prime candidates as survival genes but that requires a gene-by-gene detailed analysis. We are currently investigating the survival of *B. cenocepacia* mutants in various infection models including alfalfa (1), amoebae (44), and the nematode *Caenorhabditis elegans* (35), which represent different habitats that can all be potentially encountered by *B. cepacia* complex isolates. Elucidation of the genes required for *B. cepacia* survival in these models will provide us with a more complete picture of requirements for infection of this opportunistic pathogen.

REFERENCES

1. **Bernier, S. P., L. Silo-Suh, D. E. Woods, D. E. Ohman, and P. A. Sokol.** 2003. Comparative analysis of plant and animal models for characterization of *Burkholderia cepacia* virulence. Infect. Immun. **71:**5306–5313.

2. **Blanc-Potard, A. B., and E. A. Groisman.** 1997. The *Salmonella selC* locus contains a pathogenicity island mediating intramacrophage survival. EMBO J. **16:**5376–5385.

3. **Bottone, E. J., S. D. Douglas, A. R. Rausen, and G. T. Keusch.** 1975. Association of *Pseudomonas cepacia* with chronic granulomatous disease. J. Clin. Microbiol. **1:**425–428.

4. **Bradford, M. M.** 1976. A rapid and sensitive method for the quantitation of microgram quantities of protein utilizing the principle of protein-dye binding. Anal. Biochem. **72:**248–254.

5. **Buchmeier, N., A. Blanc-Potard, S. Ehrt, D. Piddington, L. Riley, and E. A. Groisman.** 2000. A parallel intraphagosomal survival strategy shared by *Mycobacterium tuberculosis* and *Salmonella enterica*. Mol. Microbiol. **35:**1375–1382.

6. **Burns, J. L., M. Jonas, E. Y. Chi, D. K. Clark, A. Berger, and A. Griffith.** 1996. Invasion of respiratory epithelial cells by *Burkholderia* (*Pseudomonas*) *cepacia*. Infect. Immun. **64:**4054–4059.

7. **Cerantola, S., J. Bouery, C. Segonds, N. Marty, and H. Montrozier.** 2000. Exopolysaccharide production by mucoid and non-mucoid strains of *Burkholderia cepacia*. FEMS Microbiol. Lett. **185:**243–246.

8. **Chiang, S. L., and J. J. Mekalanos.** 1998. Use of signature-tagged transposon mutagenesis to identify *Vibrio cholerae* genes critical for colonization. Mol. Microbiol. **27:**797–805.

9. **Chung, J. W., E. Altman, T. J. Beveridge, and D. P. Speert.** 2003. Colonial morphology of *Burkholderia cepacia* complex genomovar III: implications in exopolysaccharide production, pilus expression, and persistence in the mouse. Infect. Immun. **71:**904–909.

10. **Coenye, T., and P. Vandamme.** 2003. Diversity and significance of *Burkholderia* species occupying diverse ecological niches. Environ. Microbiol. **5:**719–729.

11. **Condon, C., D. Liveris, C. Squires, I. Schwartz, and C. L. Squires.** 1995. rRNA operon multiplicity in *Escherichia coli* and the physiological implications of *rrn* inactivation. J. Bacteriol. **177:**4152–4156.

12. **Corbett, C. R., M. N. Burtnick, C. Kooi, D. E. Woods, and P. Sokol.** 2003. An extracellular zinc metalloprotease gene of *Burkholderia cepacia*. Microbiology **149:**2263–2271.

13. **Corey, M., and V. Farewell.** 1996. Determinants of mortality from cystic fibrosis in Canada, 1970–1989. Am. J. Epidemiol. **143:**1007–1017.

14. **Coulter, S. N., W. R. Schwan, E. Y. Ng, M. H. Langhorne, H. D. Ritchie, S. Westbrock-Wadman, W. O. Hufnagle, K. R. Folger, A. S. Bayer, and C. K. Stover.** 1998. Staphylococcus aureus genetic loci impacting growth and survival in multiple infection environments. Mol. Microbiol. **30:**393–404.

15. **Craig, F. F., J. G. Coote, R. Parton, J. H. Freer, and N. J. Gilmour.** 1989. A plasmid which can be transferred between *Escherichia coli* and *Pasteurella haemolytica* by electroporation and conjugation. J. Gen. Microbiol. **135:**2885–2890.

16. **Darling, P., M. Chan, A. D. Cox, and P. A. Sokol.** 1998. Siderophore production by cystic fibrosis isolates of *Burkholderia cepacia*. Infect. Immun. **66:**874–877.

17. **Darwin, A. J., and V. L. Miller.** 1999. Identification of *Yersinia enterocolitica* genes affecting survival in an animal host using signature-tagged transposon mutagenesis. Mol. Microbiol. **32:**51–62.

18. **Dennis, J. J., and G. J. Zylstra.** 1998. Plasposons: modular self-cloning minitransposon derivatives for rapid genetic analysis of gram-negative bacterial genomes. Appl. Environ. Microbiol. **64:**2710–2715.

19. **Fehlner-Gardiner, C. C., T. M. Hopkins, and M. A. Valvano.** 2002. Identification of a general secretory pathway in a human isolate of *Burkholderia vietnamiensis* (formerly *B. cepacia* complex genomovar V) that is required for the secretion of hemolysin and phospholipase C activities. Microb. Pathog. **32:**249–254.

20. **Fehlner-Gardiner, C. C., and M. A. Valvano.** 2002. Cloning and characterization of the *Burkholderia vietnamiensis norM* gene encoding a multi-drug efflux protein. FEMS Microbiol. Lett. **215:**279–283.

21. **Figurski, D. H., and D. R. Helinski.** 1979. Replication of an origin-containing derivative of plasmid RK2 dependent on a plasmid function provided *in trans*. Proc. Natl. Acad. Sci. USA **76:**1648–1652.

22. **Govan, J. R., P. H. Brown, J. Maddison, C. J. Doherty, J. W. Nelson, M. Dodd, A. P. Greening, and A. K. Webb.** 1993. Evidence for transmission of *Pseudomonas cepacia* by social contact in cystic fibrosis. Lancet **342:**15–19.

23. **Govan, J. R., and V. Deretic.** 1996. Microbial pathogenesis in cystic fibrosis: mucoid *Pseudomonas aeruginosa* and *Burkholderia cepacia*. Microbiol. Rev. **60:**539–574.

24. **Govan, J. R., J. E. Hughes, and P. Vandamme.** 1996. Burkholderia cepacia: medical, taxonomic and ecological issues. J. Med. Microbiol. **45:**395–407.

25. **Guy, G. R., R. Philip, and Y. H. Tan.** 1994. Analysis of cellular phosphoproteins by two-dimensional gel electrophoresis: applications for cell signaling in normal and cancer cells. Electrophoresis **15:**417–440.

26. **Hayes, F.** 2003. Toxins-antitoxins: plasmid maintenance, programmed cell death, and cell cycle arrest. Science **301:**1496–1499.

27. **Henry, D. A., M. E. Campbell, J. J. LiPuma, and D. P. Speert.** 1997. Identification of *Burkholderia cepacia* isolates from patients with cystic fibrosis and use of a simple new selective medium. J. Clin. Microbiol. **35:**614–619.

28. **Hensel, M., J. E. Shea, C. Gleeson, M. D. Jones, E. Dalton, and D. W.**

Holden. 1995. Simultaneous identification of bacterial virulence genes by negative selection. Science **269:**400–403.

29. **Hutchison, M. L., I. R. Poxton, and J. R. Govan.** 1998. Burkholderia cepacia produces a hemolysin that is capable of inducing apoptosis and degranulation of mammalian phagocytes. Infect. Immun. **66:**2033–2039.

30. **Isles, A., I. Maclusky, M. Corey, R. Gold, C. Prober, P. Fleming, and H. Levison.** 1984. Pseudomonas cepacia infection in cystic fibrosis: an emerging problem. J. Pediatr. **104:**206–210.

31. **Jarvis, W. R., D. Olson, O. Tablan, and W. J. Martone.** 1987. The epidemiology of nosocomial *Pseudomonas cepacia* infections: endemic infections. Eur. J. Epidemiol. **3:**233–236.

32. **Johnson, W. M.** 1994. Intercontinental spread of a highly transmissible clone of *Pseudomonas cepacia* proved by multilocus enzyme electrophoresis and ribotyping. Can. J. Infect. Dis. **5:**86–88.

33. **Karlyshev, A. V., P. C. Oyston, K. Williams, G. C. Clark, R. W. Titball, E. A. Winzeler, and B. W. Wren.** 2001. Application of high-density array-based signature-tagged mutagenesis to discover novel *Yersinia* virulence-associated genes. Infect. Immun. **69:**7810–7819.

34. **Keig, P. M., E. Ingham, and K. G. Kerr.** 2001. Invasion of human type II pneumocytes by *Burkholderia cepacia*. Microb. Pathog. **30:**167–170.

35. **Köthe, M., M. Antl, B. Huber, K. Stoecker, D. Ebrecht, I. Steinmetz, and L. Eberl.** 2003. Killing of *Caenorhabditis elegans* by *Burkholderia cepacia* is controlled by the *cep* quorum-sensing system. Cell. Microbiol. **5:**343–351.

36. **Lee, B. C.** 1995. Quelling the red menace: haem capture by bacteria. Mol. Microbiol. **18:**383–390.

37. **Lefebre, M., and M. Valvano.** 2001. In vitro resistance of *Burkholderia cepacia* complex isolates to reactive oxygen species in relation to catalase and superoxide dismutase production. Microbiology **147:**97–109.

38. **Lefebre, M. D., and M. A. Valvano.** 2002. Construction and evaluation of plasmid vectors optimized for constitutive and regulated gene expression in *Burkholderia cepacia* complex isolates. Appl. Environ. Microbiol. **68:**5956–5964.

39. **Lehoux, D. E., F. Sanschagrin, and R. C. Levesque.** 1999. Defined oligonucleotide tag pools and PCR screening in signature-tagged mutagenesis of essential genes from bacteria. BioTechniques **26:**473–478, 480.

40. **Lewenza, S., B. Conway, E. P. Greenberg, and P. A. Sokol.** 1999. Quorum sensing in *Burkholderia cepacia*: identification of the LuxRI homologs CepRI. J. Bacteriol. **181:**748–756.

41. **LiPuma, J. J., S. E. Dasen, D. W. Nielson, R. C. Stern, and T. L. Stull.** 1990. Person-to-person transmission of *Pseudomonas cepacia* between patients with cystic fibrosis. Lancet **336:**1094–1096.

42. **Lutter, E., S. Lewenza, J. J. Dennis, M. B. Visser, and P. A. Sokol.** 2001. Distribution of quorum-sensing genes in the *Burkholderia cepacia* complex. Infect. Immun. **69:**4661–4666.

43. **Mahenthiralingam, E., T. Coenye, J. W. Chung, D. P. Speert, J. R. Govan, P. Taylor, and P. Vandamme.** 2000. Diagnostically and experimentally useful panel of strains from the *Burkholderia cepacia* complex. J. Clin. Microbiol. **38:**910–913.

44. **Marolda, C. L., B. Hauröder, M. A. John, R. Michel, and M. A. Valvano.** 1999. Intracellular survival and saprophytic growth of isolates from the *Burkholderia cepacia* complex in free-living amoebae. Microbiology **145:**1509–1517.

45. **Maroncle, N., D. Balestrino, C. Rich, and C. Forestier.** 2002. Identification of *Klebsiella pneumoniae* genes involved in intestinal colonization and adhesion using signature-tagged mutagenesis. Infect. Immun. **70:**4729–4734.

46. **Martin, D. W., and C. D. Mohr.** 2000. Invasion and intracellular survival of *Burkholderia cepacia*. Infect. Immun. **68:**24–29.

47. **McKevitt, A. I., S. Bajaksouzian, J. D. Klinger, and D. E. Woods.** 1989. Purification and characterization of an extracellular protease from *Pseudomonas cepacia*. Infect. Immun. **57:**771–778.

48. **Mecsas, J.** 2002. Use of signature-tagged mutagenesis in pathogenesis studies. Curr. Opin. Microbiol. **5:**33–37.

49. **Nzula, S., P. Vandamme, and J. R. Govan.** 2002. Influence of taxonomic status on the *in vitro* antimicrobial susceptibility of the *Burkholderia cepacia* complex. J. Antimicrob. Chemother. **50:**265–269.

50. **Parsons, Y. N., K. J. Glendinning, V. Thornton, B. A. Hales, C. A. Hart, and C. Winstanley.** 2001. A putative type III secretion gene cluster is widely distributed in the *Burkholderia cepacia* complex but absent from genomovar I. FEMS Microbiol. Lett. **203:**103–108.

51. **Pegues, C. F., D. A. Pegues, D. S. Ford, P. L. Hibberd, L. A. Carson, C. M. Raine, and D. C. Hooper.** 1996. Burkholderia cepacia respiratory tract acquisition: epidemiology and molecular characterization of a large nosocomial outbreak. Epidemiol. Infect. **116:**309–317.

52. **Pegues, D. A., L. A. Carson, O. C. Tablan, S. C. FitzSimmons, S. B. Roman, J. M. Miller, W. R. Jarvis, et al.** 1994. Acquisition of *Pseudomonas cepacia* at summer camps for patients with cystic fibrosis. J. Pediatr. **124:**694–702.

53. **Perry, R. D.** 1999. Signature-tagged mutagenesis and the hunt for virulence factors. Trends Microbiol. **7:**385–389.

54. **Poole, K.** 2001. Multidrug efflux pumps and antimicrobial resistance in *Pseudomonas aeruginosa* and related organisms. J. Mol. Microbiol. Biotechnol. **3:**255–264.

55. **Prince, A.** 1986. Antibiotic resistance of *Pseudomonas* species. J. Pediatr. **108:**830–834.

56. **Saini, L. S., S. B. Galsworthy, M. A. John, and M. A. Valvano.** 1999. Intracellular survival of *Burkholderia cepacia* complex isolates in the presence of macrophage cell activation. Microbiology **145:**3465–3475.

57. **Sajjan, U. S., L. Sun, R. Goldstein, and J. F. Forstner.** 1995. Cable (Cbl) type II pili of cystic fibrosis-associated *Burkholderia* (*Pseudomonas*) *cepacia*: nucleotide sequence of the *cblA* major subunit pilin gene and novel morphology of the assembled appendage fibers. J. Bacteriol. **177:**1030–1038.

58. **Sha, J., E. V. Kozlova, A. A. Fadl, J. P. Olano, C. W. Houston, J. W. Peterson, and A. K. Chopra.** 2004. Molecular characterization of a glucose-inhibited division gene, *gidA*, that regulates cytotoxic enterotoxin of *Aeromonas hydrophila*. Infect. Immun. **72:**1084–1095.

59. **Smalley, J. W., A. J. Birss, and J. Silver.** 2000. The periodontal pathogen *Porphyromonas gingivalis* harnesses the chemistry of the μ-oxo bishaem of iron protoporphyrin IX to protect against hydrogen peroxide. FEMS Microbiol. Lett. **183:**159–164.

60. **Smalley, J. W., P. Charalabous, A. J. Birss, and C. A. Hart.** 2001. Detection of heme-binding proteins in epidemic strains of *Burkholderia cepacia*. Clin. Diagn. Lab. Immunol. **8:**509–514.

61. **Sokol, P. A., P. Darling, D. E. Woods, E. Mahenthiralingam, and C. Kooi.** 1999. Role of ornibactin biosynthesis in the virulence of *Burkholderia cepacia*: characterization of *pvdA*, the gene encoding L-ornithine N^5-oxygenase. Infect. Immun. **67:**4443–4455.

62. **Speert, D. P., D. Henry, P. Vandamme, M. Corey, and E. Mahenthiralingam.** 2002. Epidemiology of *Burkholderia cepacia* complex in patients with cystic fibrosis, Canada. Emerg. Infect. Dis. **8:**181–187.

63. **Struve, C., C. Forestier, and K. A. Krogfelt.** 2003. Application of a novel multi-screening signature-tagged mutagenesis assay for identification of *Klebsiella pneumoniae* genes essential in colonization and infection. Microbiology **149:**167–176.

64. **Tomich, M., A. Griffith, C. A. Herfst, J. L. Burns, and C. D. Mohr.** 2003. Attenuated virulence of a *Burkholderia cepacia* type III secretion mutant in a murine model of infection. Infect. Immun. **71:**1405–1415.

65. **Tomich, M., C. A. Herfst, J. W. Golden, and C. D. Mohr.** 2002. Role of flagella in host cell invasion by *Burkholderia cepacia*. Infect. Immun. **70:**1799–1806.

66. **Tomlin, K. L., O. P. Coll, and H. Ceri.** 2001. Interspecies biofilms of *Pseudomonas aeruginosa* and *Burkholderia cepacia*. Can. J. Microbiol. **47:**949–954.

67. **Vandamme, P., B. Holmes, M. Vancanneyt, T. Coenye, B. Hoste, R. Coopman, H. Revets, S. Lauwers, M. Gillis, K. Kersters, and J. R. Govan.** 1997. Occurrence of multiple genomovars of *Burkholderia cepacia* in cystic fibrosis patients and proposal of *Burkholderia multivorans* sp. nov. Int. J. Syst. Bacteriol. **47:**1188–1200.

68. **Vasil, M. L., D. P. Krieg, J. S. Kuhns, J. W. Ogle, V. D. Shortridge, R. M. Ostroff, and A. I. Vasil.** 1990. Molecular analysis of hemolytic and phospholipase C activities of *Pseudomonas cepacia*. Infect. Immun. **58:**4020–4029.

69. **Vogel, H. J., and D. M. Bonner.** 1956. Acetylornithase of *Escherichia coli*: partial purification and some properties. J. Biol. Chem. **218:**97–106.

70. **Yanisch-Perron, C., J. Vieira, and J. Messing.** 1985. Improved M13 phage cloning vectors and host strains: nucleotide sequences of the M13mp18 and pUC19 vectors. Gene **33:**103–119.

71. **Zughaier, S. M., H. C. Ryley, and S. K. Jackson.** 1999. A melanin pigment purified from an epidemic strain of *Burkholderia cepacia* attenuates monocyte respiratory burst activity by scavenging superoxide anion. Infect. Immun. **67:**908–913.